

PAPER • OPEN ACCESS

## Effect of irradiation and subsequent aging on the structure of a B-1461 alloy of the Al–Cu–Li–Zn system after megaplastic deformation

To cite this article: N V Gushchina *et al* 2019 *J. Phys.: Conf. Ser.* **1393** 012087

View the [article online](#) for updates and enhancements.



**IOP | ebooks™**

Bringing together innovative digital publishing with leading authors from the global scientific community.

Start exploring the collection—download the first chapter of every title for free.

# Effect of irradiation and subsequent aging on the structure of a B-1461 alloy of the Al–Cu–Li–Zn system after megaplastic deformation

N V Gushchina<sup>1</sup>, V V Ovchinnikov<sup>1,2</sup>, F F Makhin'ko<sup>1</sup>, L I Kaigorodova<sup>3</sup> and D Yu Rasposienko<sup>3</sup>

<sup>1</sup> Institute of Electrophysics UD RAS, 106 Amundsena Str., Yekaterinburg, 620016, Russia

<sup>2</sup> Ural Federal Technical University, 19 Mira Str., Yekaterinburg, 620002, Russia

<sup>3</sup> Mikheev Institute of Metal Physics UD RAS, 18 Sofia Kovalevskaya Str., Yekaterinburg, 620990, Russia

E-mail: guscha@rambler.ru

**Abstract.** The effect of Ar<sup>+</sup> ion irradiation and subsequent prolonged aging on the microstructure and phase transformations in a B-1461 alloy (Al–Cu–Li–Zn–Mg–Zr–Sc) subjected to megaplastic deformation (MPD) has been studied by transmission electron microscopy. A mixed structure, consisting of nanocrystalline and nanofragmented regions has been found to form in the alloy upon MPD. Subsequent short-term Ar<sup>+</sup> ion irradiation ( $E = 20$  keV,  $j = 300 \mu\text{A}\cdot\text{cm}^{-2}$ ,  $F = 1.9 \times 10^{15} \text{ cm}^{-2}$ ) forms dislocation tangles, increases the nonuniform distribution and the size of structural elements, as well as volume fraction of a T<sub>2</sub>-phase (Al<sub>3</sub>CuLi<sub>5</sub>) nano and submicrocrystals heterogeneously nucleated at boundaries. Structural changes are observed at a distance of  $\sim 200 \mu\text{m}$  from the surface, which considerably exceeds the projective ion range ( $\sim 20 \text{ nm}$ ). The structure of the B-1461 alloy after MPD and subsequent irradiation under the above conditions is unstable.

## 1. Introduction

In the last years, increasing attention is paid to the creation of nanostructured metal materials to obtain unique complex of physical and mechanical properties. Megaplastic deformation (MTD) is one of the ways to achieve a nanostructured state. There are numerous experimental data [1–3] that prove the effectiveness of its application, especially in the combination with various types of heat treatment to enhance the properties of pure metals, as well as various alloys, including aluminum.

The effect of 10–40 keV gas ion beams on metastable media was shown could be an alternative to thermal annealing, resulting in similar or even more improved properties, as well as multiply accelerated process and a decreased energy consumption [4–6]. It is of interest to study the availability of ion-beam processing of alloys subjected to MPD instead of traditional annealing.

The stability of the structural components of metal alloys is known to determine the stability of their properties (including mechanical) during operation. Therefore, to investigate the structural stability of irradiated alloys previously subjected to MPD is also of interest.



The aim of this work is to use transmission electron microscopy to study the effect of accelerated ( $E = 20$  keV) argon ions and subsequent prolonged room-temperature aging on the microstructure and the phase composition of the V-1461 alloy previously subjected to MTD.

## 2. Experimental

Alloy B-1461 is a high strength, weldable, corrosion-resistant alloy developed as an alternative to a B95 alloy. Compared with the latter, it has a lower density ( $2630 \text{ kg}\cdot\text{m}^{-3}$ ), an increased elastic modulus, and an enhanced strength, and high-temperature strength. The chemical composition of the alloy is listed in table 1.

**Table 1.** Chemical composition of the V-1461 alloy, wt %.

Cu	Li	Zn	Mg	Zr	Sc	Al
2.8	1.8	0.66	0.5	0.08	0.09	Balance

V-1461 alloy samples 2 mm thick were deformed at room temperature and a pressure of 4 GPa in Bridgman anvils to 5 revolutions (angle of the anvil rotation  $\varphi = 10\pi$  rad). The thickness of the samples after deformation was  $\sim 400 \text{ }\mu\text{m}$ .

Samples subjected to MPD were irradiated with continuous  $\text{Ar}^+$  ions ( $E = 20$  keV,  $j = 300 \text{ }\mu\text{A}\cdot\text{cm}^{-2}$ ,  $F = 1.9 \times 10^{15} \text{ cm}^{-2}$ , corresponding irradiation time is 1 s) using an ILM-1 implanter equipped with a PULSAR-1M ion source based on a glow low-pressure discharge with a hollow cold cathode [7]. The temperature of the samples, controlled by thin chromel–alumel thermocouples during irradiation, did not exceed  $160^\circ\text{C}$ .

The structure and the phase composition in thin alloy foils were examined using a Tecnai 30G<sup>2</sup> Twin electron microscope at the Electron Microscopy Center of Collaborative Access of the Institute of Metal Physics, UB RAS. The foils were made from the samples by thinning them electrolytically from both sides. Thus, the initial and irradiated structures were examined at the center of the samples from a distance of  $200 \text{ }\mu\text{m}$  from both surfaces.

## 3. Details of exposure, measurements and results

First, let us consider an initial severely-deformed structure to identify the features of the irradiation effect on the MPD-deformed B-1461 alloy structure.

A structure, which is a mixture of a nanocrystalline and a nanofragmented structures, formed in the V-1461 alloy after MPD (figure 1). The first structure resulted from dynamic recrystallization [8] occupies almost the entire volume of the alloy, whereas the second one, only some regions of the sample. The diameter of recrystallized nanograins is comparable to the diameter of nanofragments and is in the range 20–50 nm. The nanograins have an equiaxed shape and either straight-line or convex–concave boundaries.

There is a contrast in the shape of arc and loops near nanograins with convex–concave boundaries, which is caused by elastic stress fields due to unbalanced surface tension. A weakly-pronounced banding with a band width of 50–100 nm is observed in some regions of the sample. According to [11], it can be explained by an MPD-induced increase in the lattice curvature.

Heterogeneously nucleated  $\text{T}_2$  ( $\text{Al}_3\text{CuLi}_5$ )-phase particles less than 5–10 nm in diameter are observed at nanograin boundaries and retained fragments of dipole boundaries.

Below are the results of the electron microscopy examination of the MPD-deformed V-1461 alloy after ion irradiation performed under the following conditions:  $E = 20$  keV,  $j = 300 \text{ }\mu\text{A}\cdot\text{cm}^{-2}$ ,  $F = 1.9 \times 10^{15} \text{ cm}^{-2}$  (irradiation time is 1 s).

After irradiation, there are uniformly distributed clusters of nanograins 30–100 nm in diameter and with close orientations in the sample volume (figure 2a). They have mainly an equiaxed shape and convex–concave boundaries; isolated dislocations are observed between them. Some regions exhibit dislocation tangles, which were not observed in the initial state. Therefore, the irradiation conditions

under consideration initiate accumulation and redistribution of lattice defects, such as dislocations. These processes proceed nonuniformly in the volume of a sample.

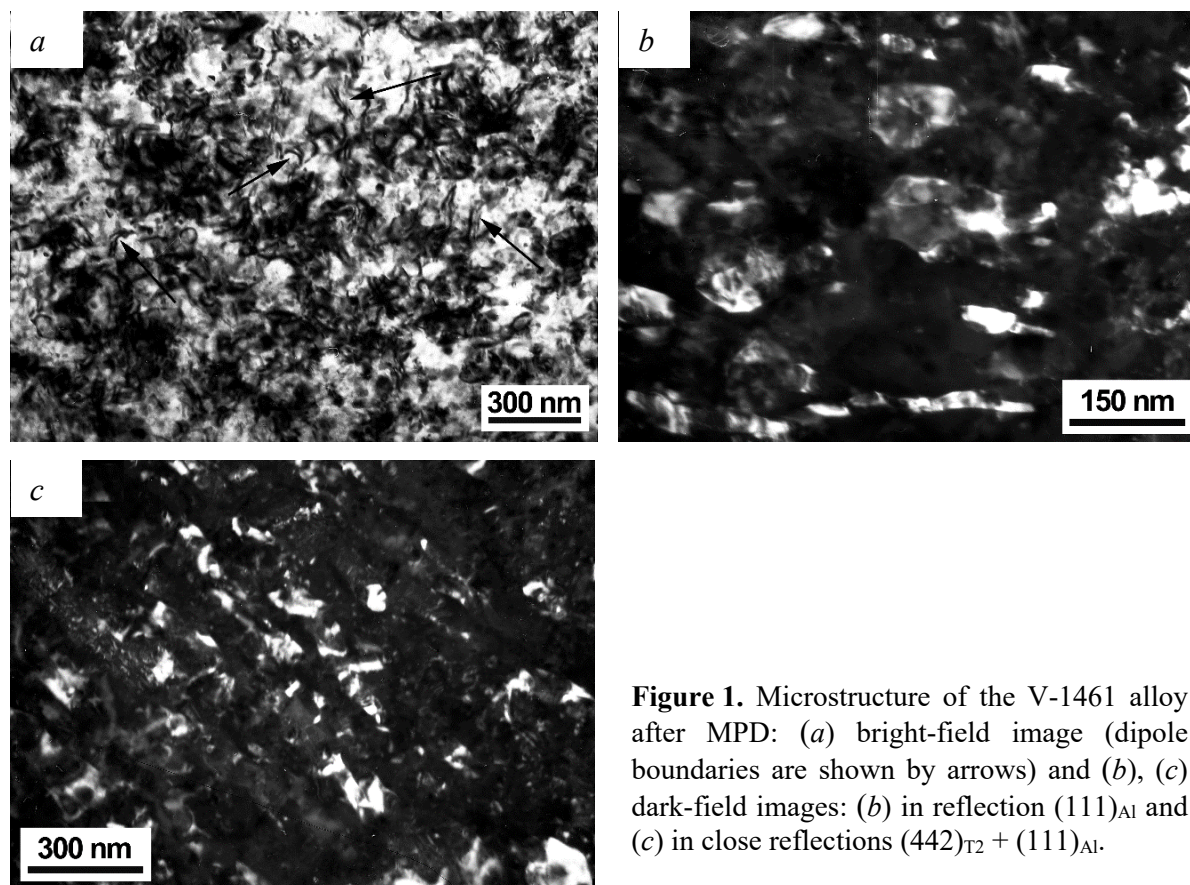


**Figure 1.** Microstructure of the V-1461 alloy after MPD: (a) bright-field image (dipole boundaries are shown by arrows) and (b), (c) dark-field images: (b) in reflection  $(111)_{\text{Al}}$  and (c) in close reflections  $(442)_{\text{T}_2} + (111)_{\text{Al}}$ .

In addition, electron microscopic images exhibit individual submicrocrystals more than 150 nm in diameter, which consist of fragments 20–30 nm in diameter (figure 2b). In some regions of the sample, structural elements are distributed anisotropically inside weakly pronounced deformation bands to 500 nm wide (figure 2c). The figures demonstrate equiaxed submicrocrystals more than 100 nm in diameter in some bands and blocks to 100 nm in length and  $\sim 50$  nm in width, in others (figure 2c). Figure 2d exemplifies one of these blocks.

The alloy retains a high-energy state after irradiation, which confirms the presence of the “fragments” of dipole boundaries (figure 2e). Such boundaries are known to be produced by MPD in Al–Li-based alloys and disappear during subsequent recrystallization [9, 10].

The irradiation under the considered conditions does not have a noticeable effect on the supersaturated solid solution decomposition of the severely deformed alloy: there are heterogeneously nucleated  $\text{T}_2$ -phase particles at nano and submicrocrystal boundaries. However, a qualitative analysis showed an increase in the density of their distribution as compared to that in the initial state (figure 2f).

Low-dose irradiation (for only 1 s) increases the heterogeneity in the distribution and the size of structural elements, whereas high-energy state is retained in the alloy. In addition, irradiation contributes to an increase in the volume fraction of the  $\text{T}_2$  phase.

Let us further consider the results of the electron microscopic examination of the samples after irradiation and prolonged aging at room temperature.

Analysis of electron microscopic images of the alloy V-1461 sample after long-term aging (for 4 months) showed that irradiation-induced dislocation tangles completely disappears after aging. As a

result, an almost uniform nano and submicrocrystalline structure with uniformly distributed structural elements 100–150 nm in size is formed in the entire sample volume (figure 3a).

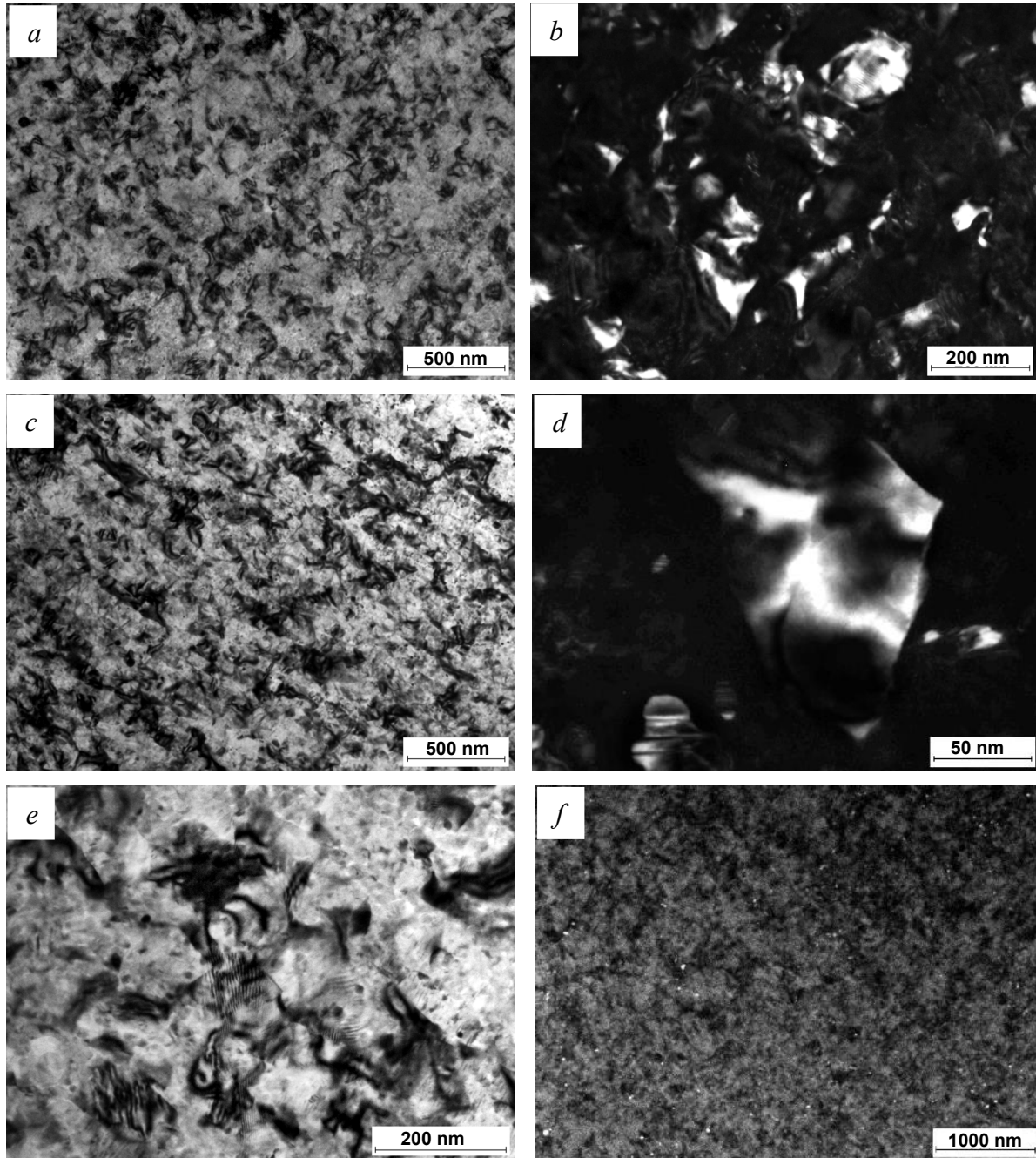


**Figure 2.** Microstructure of the V-1461 alloy after MPD and  $\text{Ar}^+$  ion irradiation ( $E = 20$  keV,  $j = 300 \mu\text{A}\cdot\text{cm}^{-2}$ ,  $F = 1.9 \times 10^{15} \text{ cm}^{-2}$ ): (a), (c), (e) – bright-field images and (b), (d), (f) – dark-field images: (b), (d) in reflection  $(200)_{\text{Al}}$  and (f) –  $(530)_{\text{T2}}$ .

A comparison of alloy structures after irradiation and aging suggests that the aging of the irradiated alloy makes the grain structure coarser and decreases the size nonuniformity. After aging, nano and submicrocrystals possess both equilibrium rectilinear and nonequilibrium convex–concave boundaries (figure 3a). A deformation contrast in the shape of loops or arcs is observed near the latter (figure 3b). This contrast is associated with the nonequilibrium elastically distorted lattice state near the convex–



concave boundaries of nanograins [2]. A contrast pattern in the dark-field images of the alloy after aging indicates the predominance of nanograins with nonequilibrium boundaries (figure 3c). Despite the fact that there are no dislocation tangles, but a uniform grain structure has formed, a complete transition of the irradiated state to a low-energy recrystallized one does not occur during aging which confirms that the dipole boundary “fragments” have been retained (figure 3d).

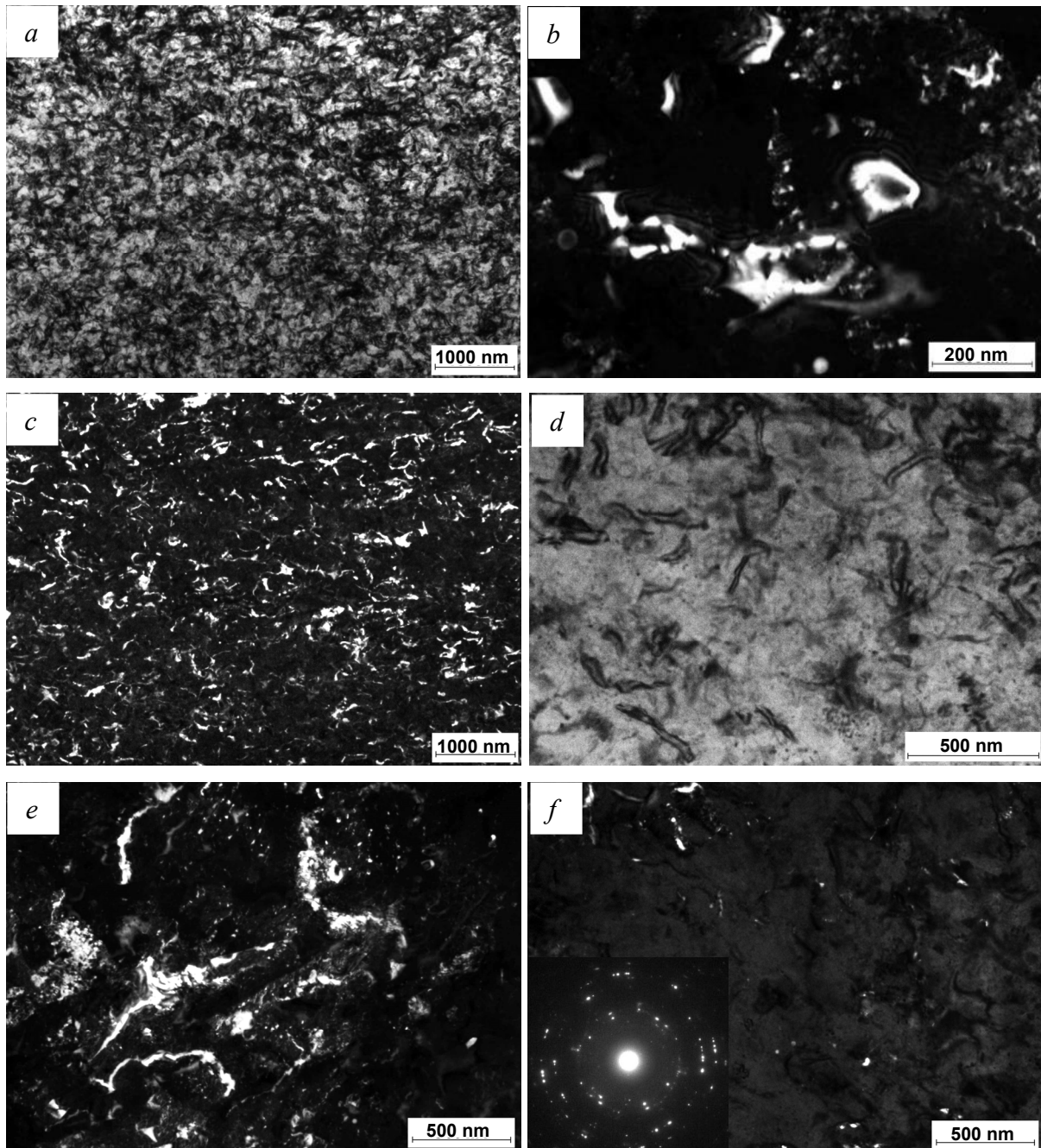


**Figure 3.** Microstructure of the V-1461 alloy after MPD and  $\text{Ar}^+$  ion irradiation ( $E = 20$  keV,  $j = 300 \mu\text{A}\cdot\text{cm}^{-2}$ ,  $F = 1.9 \times 10^{15} \text{ cm}^{-2}$ ) and aging: (a), (d) bright-field images and (b), (c), (e), (f) dark-field images: (b), (c) in reflection  $(200)_{\text{Al}}$  and (e), (f)  $(530)_{\text{T}_2}$ , and (f) electron diffraction pattern.

Aging does not affect the phase composition of the alloy: in addition to matrix reflections, there are reflections of the  $\text{T}_2$  ( $\text{Al}_3\text{CuLi}_5$ ) phase in the electron diffraction patterns (figure 3e).  $\text{T}_2$  particles are

observed in the bright-field and dark-field images (figures 3e and 3f). Analysis revealed the size bimodality of these particles. For example, particles less than 10 nm in diameter, which are uniformly distributed along grain boundaries can be seen in figure 3e are shown, and particles ~20–30 nm in diameter, in figure 3f are shown.

A comparison of the irradiated alloy before and after aging demonstrates an increase in the density of T<sub>2</sub> particles. This indicates that aging promotes two processes simultaneously: coagulation of precipitates observed in the irradiated alloy and the nucleation and growth of new particles. Coarser particles resulted from the coagulation of irradiation-induced T<sub>2</sub>-phase particles. Fine particles nucleated during the aging process.

#### 4. Conclusions

Transmission electron microscopy showed that megaplastic deformation ( $P = 4$  GPa,  $\varphi = 10\pi$  rad) formed a mixed structure in the V-1461 alloy, which included the regions of nanofragmented structure, along with the nanocrystalline regions occupying the most part of the sample volume.

Short-term (for 1 s) 20-keV Ar<sup>+</sup> ion irradiation ( $j = 300 \mu\text{A}\cdot\text{cm}^{-2}$ ,  $F = 1.9 \times 10^{15} \text{ cm}^{-2}$ ) of the V-1461 alloy after MPD formed dislocation tangles, increased the nonuniform distribution and the size of structural elements, as well as the volume fraction of the T<sub>2</sub> phase (Al<sub>3</sub>CuLi<sub>5</sub>) heterogeneously nucleated at nano and submicrocrystal boundaries. These processes occur in the surface layer not less than 200 μm thick, which significantly exceeds the projective ranges of argon ions in the alloy (~20 nm).

The structure of the B-1461 alloy after MPD and subsequent irradiation under the above conditions was shown to be unstable. Subsequent room-temperature aging resulted in the annihilation of irradiation-induced dislocations tangles. In addition, size uniformity enhanced, grains and T<sub>2</sub>-phase particles became coarser, and the volume fraction of the T<sub>2</sub>-phase increased.

#### Acknowledgments

This work was supported in part by RFBR grant No. 18-08-00942-A.

#### References

- [1] Gleiter H 1989 *Progress in Materials Science* **33** 223
- [2] Valiev R Z and Aleksandrov I V 2007 *Volume Nanostructured Metal Materials: Synthesis, Structure, and Properties* (Moscow: Akademkniga)
- [3] Andrievskii R A and Ragulya A V 2005 *Nanomaterials* (Moscow: Academia)
- [4] Ovchinnikov V V et al 2010 *Russian metallurgy (Metally)* **3** 207
- [5] Ovchinnikov V V et al 2017 *Physics of Metals and Metallography* **118** 150
- [6] Ovchinnikov V V 2018 *Surface and Coating Technology* **355** 65
- [7] Gavrilov N V, Mesyats G A, Nikulin S P, Radkovskii G V, Eklind A and Perry A J 1996 *J. Vac. Sci. Technol. A* **14** 1050
- [8] Kaigorodova L I, Rasposienko D Y, Pushin V G, Pilyugin V P and Smirnov S V 2018 *Physics of Metals and Metallography* **119** 161
- [9] Kaigorodova L I, Rasposienko D Y, Pushin V G, Pilyugin V P and Smirnov S V 2015 *Physics of Metals and Metallography* **116** 346
- [10] Kaigorodova L I, Pushin V G, Rasposienko D Y and Pilyugin V P 2011 *Physics of Metals and Metallography* **111** 74
- [11] Ditenberg I A et al 2011 *Technical Physics. The Russian Journal of Applied Physics* **56** 815